



## YIELD-LINE ANALYSIS BY SEQUENTIAL LINEAR PROGRAMMING

DAVID JOHNSON

Department of Civil and Structural Engineering, The Nottingham Trent University,  
Burton Street, Nottingham NG1 4BU, U.K.

(Received 3 December 1993; in revised form 4 August 1994)

**Abstract**—The rigid-plastic yield-line analysis of isotropically reinforced concrete slabs under uniformly distributed loading is developed as the lower bound form of a linear programming formulation. The analysis is extended to consider geometric variation of chosen yield-line patterns by the technique of sequential linear programming. Linearized geometric sensitivities for use with the sequential process are developed analytically. The geometric variation algorithm is shown to be effective for the determination of collapse loads and modes, although the evaluation of collapse geometries is often of a lower order of accuracy than that of collapse load determination. Direct generation of critical collapse modes is not generally possible although an indication of more significant modes may be obtainable in some instances.

### INTRODUCTION

#### *Background*

Perhaps surprisingly, the yield-line analysis of plates and slabs [see Wood (1961)] has proved less amenable to automation than elastic plate analysis by the finite element and other numerical approaches. The problems to be solved in automating yield-line analysis may be listed as:

- (a) the determination of the collapse load factor for a specified yield-line pattern;
- (b) the identification of the critical yield-line pattern from a number of specified alternative collapse modes;
- (c) the determination of the critical geometry for a specified yield-line topology;
- (d) the direct generation of critical collapse modes.

Thus, for the simple rectangular slab shown in Fig. 1(a), it must be possible to determine the collapse load for each of the potential mechanisms shown on the half-slab of Fig. 1(b) and to identify which is the governing mechanism. In addition, for mechanisms 1 and 3, variation of the indicated geometrical variables must be examined to refine and confirm the identification of the critical mode. Finally, the competing modes or, ideally, the critical mode directly, should be automatically generated.

The determination of collapse load factors for specified yield-line systems has been achieved by the automation of hand approaches [see e.g. Dickens and Jones (1988)], but this tends to be restricted to a limited range of boundary conditions and to require separate consideration of competing yield-line patterns. A more general, machine orientated approach is to apply linear programming techniques [see Anderhaggen and Knopfel (1975); Munro and Da Fonseca (1978)]. In this method, the slab is subdivided into triangular regions and yield may occur along any of the boundaries of the triangulation. The collapse mechanism does not need to be specified initially since the methodology will identify the critical yield-line pattern. The patterns identified, however, are necessarily restricted by the selected subdivision, since only mechanisms which can be constructed from the chosen triangulation will be examined. Also, for a given mechanism, only the geometry specified by the subdivision is considered. Variation of mechanism geometry has been attempted by Jennings *et al.* (1994), using a geometrical optimisation technique in conjunction with the

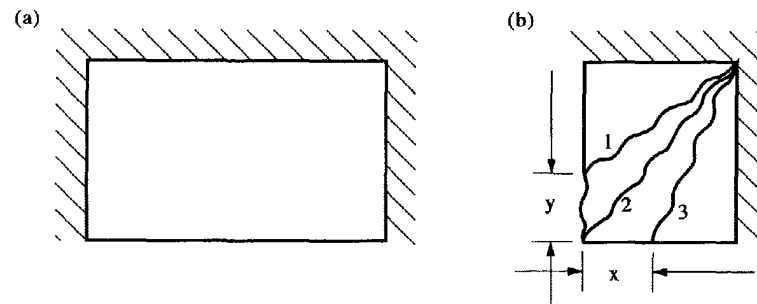


Fig. 1. (a) Rectangular slab; (b) yield-line systems for the half-slab.

linear programming algorithm. However, this approach met with convergence difficulties even in the case of a simple regular slab.

### Objectives

The present paper extends the linear programming formulation of yield-line analysis to the consideration of variable mechanism geometry by the use of sequential linear programming. This conveniently permits the repetitive use of the programming procedure already used for the fixed geometry analysis and has proved to be an effective solution for a range of test analyses, a selection of which are provided as examples later in the paper. The problem of automated mechanism selection is not explicitly tackled, but indications are given of ways in which the proposed formulation may be used to assist in the generation of critical mechanism topologies.

The linear programming approach readily allows all commonly employed support conditions to be modelled and any edge geometry may be considered. In the interests of simplicity, isotropic reinforcement and uniformly distributed loading are considered in the theoretical development presented herein, although extensions to a direct treatment of orthotropic reinforcement and point or line loading could be readily achieved. Regular orthotropic situations may be treated indirectly by use of the "affine" [see Wood (1961)] theorems of yield-line analysis and point and line loading may also be tackled indirectly by using suitable, equivalent, uniform patch loads.

## THEORY

### *Yield-line analysis by linear programming*

Yield-line analysis by linear programming has generally [see e.g. Munro and Da Fonseca (1978); Jennings *et al.* (1994)] been effected using nodal displacement ( $w$ ) and edge rotation ( $\theta$ ) variables. However, it has been recognised that a *dual* formulation is possible [see Anderhaggen and Knopfel (1975); Munro and Da Fonseca (1978)] which employs edge moments ( $m$ ) and nodal forces ( $f$ ) as the fundamental quantities. This latter formulation has been preferred as being perhaps more straightforward conceptually. It may also be more computationally efficient, when used with the "upper bounded" [see Garvin (1960)] form of the linear programming algorithm.

The slab to be analysed is meshed into triangular regions, a typical such region being shown in Fig. 2(a). If, in Fig. 2(b), the moments per unit length, assumed uniform, are  $m_1, m_2, m_3$  along the edges of the triangle and the applied nodal forces are  $f_1, f_2, f_3$ , then, under the action of a uniformly distributed load of intensity  $q$  at load factor  $\lambda$ , the equilibrium conditions for the region are

$$\mathbf{C}^e \mathbf{m}^e = \lambda \mathbf{f}^e \quad (1)$$

where

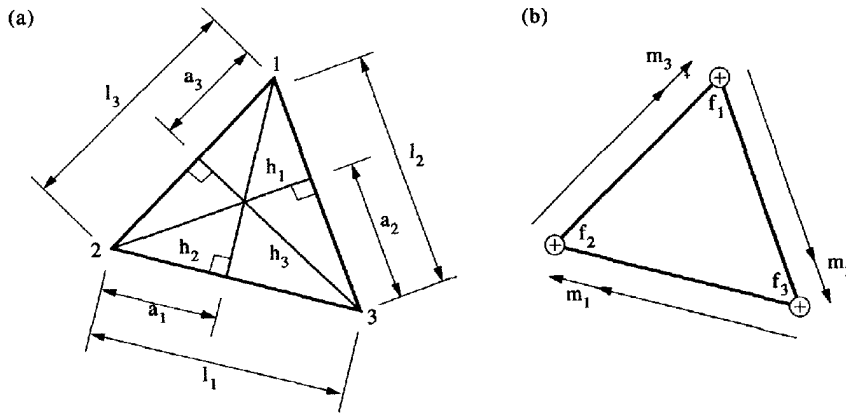


Fig. 2. (a) Triangular region; (b) statics of region.

$$\mathbf{m}^e = \{m_1, m_2, m_3\}^t; \quad \mathbf{f}^e = \left\{ \frac{q\Delta}{3}, \frac{q\Delta}{3}, \frac{q\Delta}{3} \right\}^t$$

and

$$\mathbf{C}^e = \begin{bmatrix} -\left(\frac{a_1}{h_1} + \frac{a_2}{h_2}\right) & \frac{a_2}{h_2} & \frac{a_1}{h_1} \\ \frac{a_2}{h_2} & -\left(\frac{a_2}{h_2} + \frac{a_3}{h_3}\right) & \frac{a_3}{h_3} \\ \frac{a_1}{h_1} & \frac{a_3}{h_3} & -\left(\frac{a_3}{h_3} + \frac{a_1}{h_1}\right) \end{bmatrix}$$

in which

$$a_1 = \frac{l_1^2 - l_2^2 + l_3^2}{2l_1}, \quad h_1 = \frac{(y_1 - y_2)(x_3 - x_2) - (x_1 - x_2)(y_3 - y_2)}{l_1} \quad \text{and} \quad \Delta = \frac{h_1 l_1}{2}$$

(other values of  $a, h$  are obtained by cyclic suffix permutation).

If there are  $n_j$  nodes at which normal displacement is allowed and  $n_b$  moment-resisting boundaries, then, summing contributions from all the  $n_e$  regions to the forces at all the  $n_j$  nodes, due to the moments along the  $n_b$  boundaries, gives the complete set of equilibrium conditions:

$$\mathbf{Cm} = \lambda \mathbf{f} \tag{2}$$

where

$$\mathbf{m} = \{m_1, \dots, m_{n_b}\}^t \quad \text{and} \quad \mathbf{f} = \{f_1, \dots, f_{n_j}\}^t.$$

Under isotropic conditions, all the moments/unit length will be bounded by the constant plastic moments of resistance/unit length in positive and negative bending,  $m^+$  and  $m^-$ , respectively, such that

$$\mathbf{u}m^- \leq \mathbf{m} \leq \mathbf{u}m^+ \tag{3}$$

where  $\mathbf{u} = \{1, \dots, 1\}^t$  is the unit vector.

Equations (2) and (3) represent the conditions of equilibrium and yield, respectively, for the slab. By the lower bound theorem of plasticity, the collapse solution may therefore be obtained by maximising the load factor  $\lambda$  subject to the linear conditions expressed by the above equations. This is a linear programming problem and may be solved by standard techniques [see Garvin (1960)].

#### *Displacement and rotation solution*

The linear programming solution will provide the collapse load factor and the boundary moment values at collapse. To obtain the yield-line pattern at collapse, it is necessary to determine the rotations along the specified boundaries, since only boundaries with non-zero rotations will represent yield-lines. Boundary rotations  $\theta$  and nodal displacements  $\mathbf{w}$  may be determined by application of the "dual" properties of linear programming [see Munro and Da Fonseca (1978) and Garvin (1960)] or may be established from the following structural considerations.

The geometric relationship which is contragredient to the equilibrium condition of eqn (2) is

$$\theta = \mathbf{C}'\mathbf{w}. \quad (4)$$

At the conclusion of the linear programming process, the load factor and  $n_j - 1$  of the boundary moments  $\mathbf{m}$ , will be "basic" variables and, by definition, will be neither at their upper nor their lower bound. Assuming rigid-plastic behaviour, it follows that there can be no rotation along the boundaries corresponding to the  $\mathbf{m}$ . Equation (4) may therefore be extended to

$$\begin{Bmatrix} \mathbf{0} \\ \theta_p \\ 1 \end{Bmatrix} = \begin{Bmatrix} \mathbf{C}'_r \\ \mathbf{C}'_p \\ \mathbf{u}' \end{Bmatrix} \mathbf{w}. \quad (5)$$

In eqn (5), the lowest relationship is a scaling which reflects the relative nature of the displaced shape of the slab. The relative displacements may be obtained from the upper and lower relationships of eqn (5) as

$$\mathbf{w} = \begin{bmatrix} \mathbf{C}'_r \\ \mathbf{u}' \end{bmatrix}^{-1} \begin{Bmatrix} \mathbf{0} \\ 1 \end{Bmatrix}. \quad (6)$$

The rotations along the potential yield-lines then follow from the second relationship of eqn (5).

#### *Variable yield-line geometry*

If variation in yield-line geometry is considered, then eqn (2) becomes non-linear since both  $\mathbf{C}$  and  $\mathbf{f}$  are geometry dependent. The technique of sequential linear programming relies on an iterative process in which linearised approximations are used in any particular iteration. Equation (2) may be linearised by replacing each term by its first-order Taylor series approximation to give

$$\dot{\mathbf{C}}\mathbf{m} + \mathbf{J}_{C_x}\Delta_x = \dot{\lambda}\mathbf{f} + \dot{\lambda}\mathbf{J}_{f_x}\Delta_x \quad (7)$$

where  $\Delta_x = \mathbf{x} - \dot{\mathbf{x}}$  and  $\mathbf{x}$  is the geometric variable vector.

In eqn (7),  $\dot{\phantom{x}}$  indicates evaluation with respect to the current geometry, and such terms therefore remain constant during the succeeding iteration. Also, the Jacobian matrices  $\mathbf{J}_{C_x}$  and  $\mathbf{J}_{f_x}$  are given by

$$\mathbf{J}_{Cx} = \left[ \dots, \frac{\partial \dot{C}}{\partial x_i} \dot{\mathbf{m}}, \dots \right] \quad \text{and} \quad \mathbf{J}_{f_x} = \left[ \dots, \frac{\partial \dot{\mathbf{f}}}{\partial x_i}, \dots \right]. \quad (8)$$

The derivatives required for the construction of the Jacobian matrices of eqn (8) may be obtained analytically and appropriate expressions are provided in the Appendix. The previous equilibrium constraints, eqn (2), are replaced by eqn (7) and the linear programming solution is repeated. At the conclusion of the programming procedure, the "objective function" values corresponding to the geometric variables  $\Delta_x$  will indicate the sense in which the variables need to be amended in order to appropriately modify the load factor. At this stage, reductions in the load factor are sought since geometric variation represents an upper bounded solution.

The magnitudes of the changes to the geometric variables cannot be obtained from a linear solution and must be enforced by the imposition of suitable bounds. Clearly, the geometric variables will need to be constrained by lower bounds  $\bar{\mathbf{x}}$  and upper bounds  $\bar{\bar{\mathbf{x}}}$  which are designed to ensure that the confines of the slab and its basic topology are not altered. In addition, however, geometric variation at any iteration must be limited so that unacceptable linearization errors do not occur. The errors incurred by geometric linearization have been taken to be dependent on the fineness of the local triangulation, on the premise that the linearization will remain effective if all amendments to the areas of the triangular regions and the orientations of the boundaries remain within a specified tolerance. Thus if, for all the boundaries meeting at node  $i$ , the average, absolute value of the projection of the triangle edges in respect of geometric variable  $x_i$  is  $\bar{x}_i$ , then the bounds are given by

$$\max(\bar{\mathbf{x}}, \mathbf{x} - \lceil (1 - \beta_i) \rceil \bar{\mathbf{x}}) < = \mathbf{x} \leq \min(\bar{\bar{\mathbf{x}}}, \mathbf{x} + \lceil (1 + \beta_i) \rceil \bar{\mathbf{x}}) \quad (9)$$

where  $\lceil (1 \pm \beta_i) \rceil$  are the diagonal *move limit* matrices.

All the individual move limits  $\beta_i$  are initially taken to be 0.25 to allow reasonable geometric change but not so as to produce undue distortion of the subdivision. Subsequently, the move limits are expanded such that  $\beta_i = 1.1\beta_i$  if the three previous iterations indicate a consistent direction of variation in a given parameter. If the three previous iterations indicate an oscillation in a parameter, this is taken as an indication that a critical value has been passed and the bounds are tightened by setting  $\beta_i = 0.5\beta_i$  so that the solution is driven towards the critical value.

Convergence of the sequential linear programming process is based on successive changes in load factor. A stipulation that none of the latest three load factor values vary by more than 0.1% has generally been found to be effective in ensuring reasonable accuracy, and in preventing accidental termination due to coincidentally similar successive values.

#### Linkage of geometric variables

To preserve the form of a specified yield-line pattern under geometric variation, it is often necessary to link geometric variables to each other. One straightforward requirement is that one geometric parameter  $x_j$  remains equal to another parameter  $x_i$ . In such a case, substitution of  $\Delta_{x_j}$  for  $\Delta_{x_i}$  in eqn (7) will suffice. A more demanding requirement is that a number of nodes should be constrained to remain on a straight line. The representation used in this case is to make two of the nodes on the line "defining" nodes, which may have up to two geometric variation parameters each. The remaining nodes then become "intermediate" and have a maximum of one geometric parameter each, which is taken to be  $\mu$ , defined such that the coordinates of an intermediate point,  $x, y$ , are related to the coordinates of the line's defining points,  $x_1, y_1$  and  $x_2, y_2$ , by

$$x = \mu(x_2 - x_1) + x_1 \quad \text{and} \quad y = \mu(y_2 - y_1) + y_1. \quad (10)$$

Since eqn (10) contains product terms in the variables  $\mu, x_1, x_2$ , it represents a pair of non-linear functions. Appropriate linearizations are therefore required, which take the form

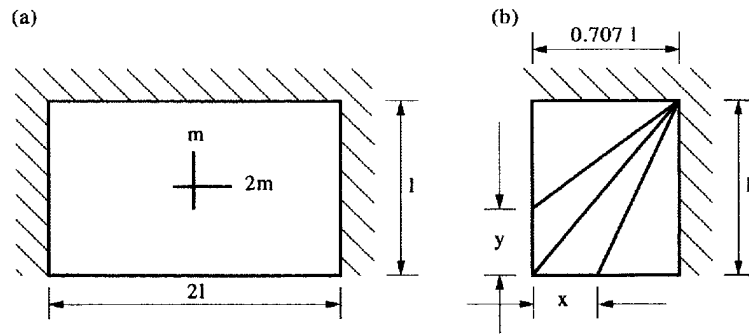


Fig. 3. (a) Rectangular orthotropic slab; (b) half-slab model.

$$\begin{aligned} \Delta_x &= (\dot{x}_2 - \dot{x}_1)\Delta_\mu + (1 - \dot{\mu})\Delta_{x_1} + \dot{\mu}\Delta_{x_2} \\ \Delta_y &= (\dot{y}_2 - \dot{y}_1)\Delta_\mu + (1 - \dot{\mu})\Delta_{y_1} + \dot{\mu}\Delta_{y_2}. \end{aligned} \tag{11}$$

Equations (11) allow the coordinates of an intermediate node to be linked to the coordinates of the line's defining joints and the parameter  $\mu$ . Should it be required to keep one of an intermediate node's coordinates constant, then the variation of the other coordinate may be expressed solely in terms of the defining positions since if  $\Delta_y = 0$ , say, then, from the second of eqns (11),

$$\Delta_\mu = -\frac{(1 - \dot{\mu})}{(\dot{y}_1 - \dot{y}_2)} \Delta_{y_1} - \frac{\dot{\mu}}{(\dot{y}_1 - \dot{y}_2)} \Delta_{y_2}. \tag{12}$$

Hence, from the first of eqns (11),

$$\Delta_x = -\frac{(\dot{x}_2 - \dot{x}_1)(1 - \dot{\mu})}{(\dot{y}_1 - \dot{y}_2)} \Delta_{y_1} - \frac{\dot{\mu}(\dot{x}_2 - \dot{x}_1)}{(\dot{y}_1 - \dot{y}_2)} \Delta_{y_2} + (1 - \dot{\mu})\Delta_{x_1} + \dot{\mu}\Delta_{x_2}. \tag{13}$$

EXAMPLES

The examples given are, for ease of presentation, restricted to slabs having relatively straightforward geometries, in which advantage of symmetry can be taken to simplify the problem. Nevertheless, a range of boundary conditions is examined and some demanding situations in respect to competing modes are elucidated. The treatment of more extensive and irregular slab systems poses no novel theoretical difficulties and such systems are currently being investigated. In each case, the sequential linear programming technique has been used to evaluate the uniformly distributed collapse load  $q_u (= \lambda q)$ . For numerical purposes, the generalised uniformly distributed load  $q$ , the generalised length  $l$ , and the generalised moment of resistance/unit length  $m$  were all taken to be unity. For such values, it follows that the quoted numerical collapse load values  $q_u$  are equal to the relevant load factors  $\lambda$  obtained from the programming solutions.

*Rectangular orthotropic slab*

The orthotropic rectangular slab shown in Fig. 3(a) is simply supported on three sides and free on the remaining side. Using symmetry and the affine theorems, the isotropic half-slab shown in Fig. 3(b) may be considered. The triangulation shown encompasses the three possible modes of collapse, which have been previously illustrated [Fig. 1(b)]. The geometric variables are taken to be  $x$  and  $y$ . Collapse is, in fact, by mode 1 of Fig. 1(b) and the variation in the geometric parameters and collapse load during the course of the iterations

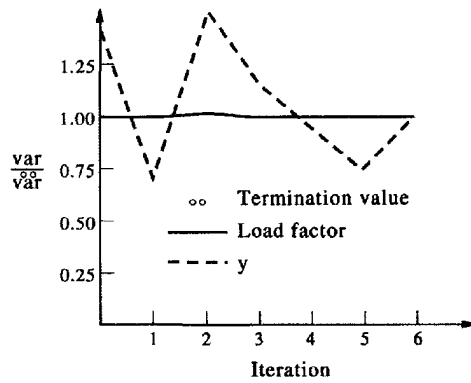


Fig. 4. Solution graph for a rectangular orthotropic slab.

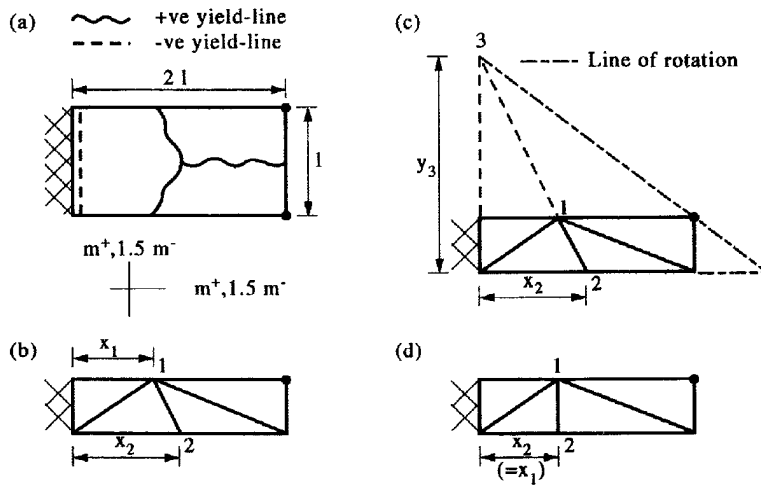


Fig. 5. (a) Twin column supported cantilever slab; (b-d) subdivisions for analyses of the half-slab.

are shown in Fig. 4. It may be seen from Fig. 4 that, although the ultimate load converges rapidly to a value of  $8.87 m/l^2$ ,  $y$  does not converge effectively, illustrating the typical insensitivity of ultimate loads to geometrical change in regions of sagging bending. Further evidence of this is provided by the minor reduction achieved from the original ultimate load of  $8.94m/l^2$  by significant geometric change.

*Twin column supported cantilever slab*

The cantilever slab shown in Fig. 5(a) is supported by corner columns at its free corners and the column heads are presumed adequate to prevent local collapse. The anticipated form of the yield-line pattern is as shown. Figure 5(b) shows the half-slab analysed, together with the triangulation adopted. The geometric variables used were the coordinates  $x_1$  and  $x_2$ . The resulting analysis, recorded in the first row of Table 1, does not represent a converged solution and, indeed, the collapse load at termination  $\bar{q}_u$  is actually greater than that

Table 1. Twin column supported cantilever slab

Figure	$\bar{x}_1 x_l \dagger$	$\bar{x}_2 x_l$	$\bar{x}_1 x_l$	$\bar{x}_2 x_l$	$\bar{x}_1 x_l \ddagger$	$\bar{x}_2 x_l$	$\bar{q}_u x m / l^2$	$\bar{q}_u x m / l^2$	Iterations
5(b)	0.75	1.00	1.90	0.10	1.47	1.12	5.186	5.217	8
5(b)	0.75	1.75	1.25	1.25	1.25	1.25	7.483	3.333	4
5(c)	0.75	1.00	—	0.10	1.00	1.00	5.186	3.497	27
5(d)	0.75	0.75	1.90	0.10	1.24	1.24	4.133	3.332	8

† indicates initial value; ‡ indicates termination value.

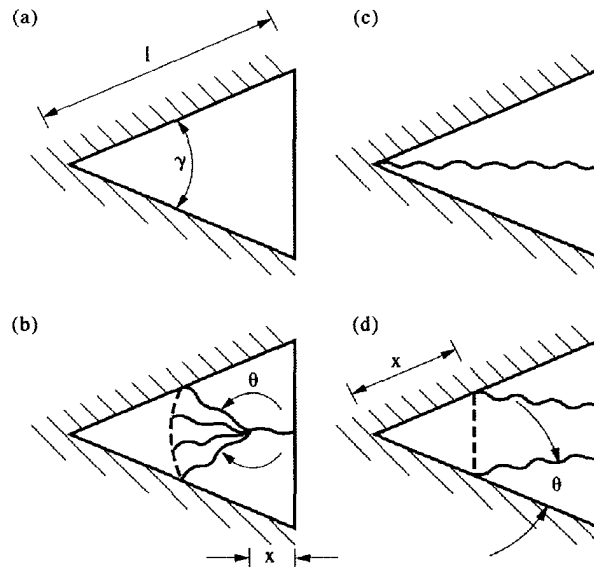


Fig. 6. (a) Isosceles triangular slab with free edge; (b-d) possible collapse mechanisms for the slab.

associated with the initial geometry  $q_u$ . This situation has arisen since the liberal limits allowed for the geometrical variables ( $\bar{x}_1, \bar{x}_2$ ) have allowed  $x_1$  to exceed  $x_2$  and have hence resulted in a different collapse mode to that originally envisaged [Fig. 5(a)]. Clearly, as indicated in the second row of Table 1, this can be readily rectified by the adoption of more appropriate bounds. Another approach would be to use the linear linkage facility, with node 1 becoming an intermediate position in relation to the defining nodes 2 and 3 [Fig. 5(c)], so that the geometric variables are  $x_2$  and  $y_3$ . As the third row of Table 1 shows, this analysis is slow to converge, but does indicate that the critical collapse mode requires  $x_1$  and  $x_2$  to be equal, something that is not strictly possible under the linear linkage arrangement.

To ensure that the critical mode is included, equality of  $x_1$  and  $x_2$  can be enforced [Fig. 5(d)]. Such a specification converges closely to the analytical solution, given by Johansen (1972), of  $x_1 = x_2 = 1.23l$  and  $q_u = 3.333 m/l^2$ . This example therefore illustrates the need for the selected subdivision and associated bounds to be capable of modelling exactly the critical yield-line pattern. Failure to model a valid mechanism in the liberally bounded case led to non-convergence, while the inability of the linearly linked case to precisely represent the actual collapse pattern resulted in slow convergence to a non-critical geometric solution, although it did indicate the nature of the critical collapse mode.

#### *Isosceles triangle with free edge*

The triangular slab shown in Fig. 6 is isosceles and subtends an angle of  $\gamma$  between two simply supported sides, being free on the opposite side. It has been shown by Wood (1961) that such a slab can exhibit three distinct collapse modes and this problem is therefore expected to provide a demanding example in respect to the ability of the sequential linear programming process's ability to discriminate between competing modes. The triangulation shown in Fig. 7 was used, based on a half-slab model. The geometrical parameters were taken to the positions of nodes 2, 3, 4 and 6, restricted so that the nodes remained on their respective boundaries. The experience of the previous example was utilised to ensure that all three possible collapse modes can be modelled by this one triangulation, although the fan mechanism of Fig. 6(b) is only coarsely represented by an approximating "corner lever" system. The results of analyses employing three values of negative to positive reinforcement ratio and two values of corner angle  $\gamma$  are given in Table 2. For ease of comparison with solutions presented by Wood (1961), the collapse mode geometries in Table 2 are specified in terms of the parameters  $x$  and  $\theta$ , which are defined for modes (b) and (d) in Figs 6(b) and (d), respectively.



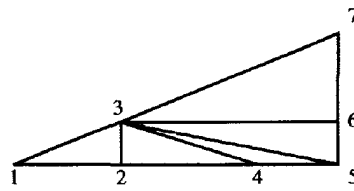


Fig. 7. Subdivision for isosceles triangular slab analysis.

Table 2 shows that the sequential programming process does manage to discriminate between the various modes in all but one case (the  $90^\circ$  triangle with 0.5 reinforcement ratio). It may also be noted that the various modes are not strongly sensitive to geometric change, there being relatively minor differences between initial and final collapse loads, despite the substantial geometric alterations which sometimes occur. In one case (the  $45^\circ$  triangle with zero reinforcement ratio), the numerical collapse load result diverges somewhat from the closed-form solution, which can probably be attributed to the rather crude fan representation involved in the relevant mode. Inadequate fan representation may also be the cause of the mistaken mode identification referred to above. The lack of geometric sensitivity, coupled with the coarse fan representation, has resulted in occasional imprecision in the critical geometries identified, this being particularly evident in the  $45^\circ$  triangle, zero reinforcement ratio analysis.

## CONCLUSIONS

(a) Linear programming provides an efficient algorithm for the determination of collapse load factors for specified yield patterns.

(b) Sequential linear programming effectively extends the formulation to include geometric variables and permits the determination of critical collapse loads. The associated critical geometries are likely to be less accurately evaluated than the associated collapse loads, however, partly due to the nature of the linearized process and partly due to the insensitivity of collapse loads to variation of yield-line geometry in regions of sagging bending. It follows that geometric variation is only likely to have a significant effect on collapse loads in the case of yield-line systems which are geometrically variable in, or close to, regions of hogging bending.

(c) The formulation will identify critical yield-line topologies from a number of specified alternatives. However, it is essential that the triangulation and bounds selected are such that the critical mechanism is incorporated and are also such that geometric alterations do not produce topological change.

Table 2. Isosceles triangle with free edge

$\gamma$ degrees	$\frac{m^-}{m^+}$	$\bar{x} \times l$	$\bar{y} \times l$	$\hat{\theta}$ degrees	$\hat{\theta}$ degrees	$\hat{q}_u \times m/l^2$	$\hat{q}_u \times m/l^2$	Mode (Fig. 6)	Iterations
45	0	0.224	0.125 (0.1)†	34.5	40 (60)	31.9	31.3 (30.1)	(b) (b)	7
	0.5	0	0	22.5	22.9	34.04	34.03	(b)	4
	1	0	0 (0)	22.5	19 (15)	35.9	35.8 (35.3)	(b) (b)	5
90	0	0.283	0.289 (0.30)	45	56 (56)	10.69	10.18 (10.17)	(d) (d)	8
	0.5	—	— (0.10)	—	— (17)	12	12 (11.70)	(c) (b)	3
	1	—	— (—)	—	— (—)	12	12 (12)	(c) (c)	3

† Bracketed values are from Wood (1961).

(d) The sequential linear programming approach does not directly generate likely critical collapse modes. However, in some circumstances, results from a geometrical optimization will indicate possible critical mechanisms which can be investigated by further analyses using modified triangulations and bounds.

## REFERENCES

- Anderhaggen, E. and Knopfel, H. (1975). Berechnung der Traglast von Stahlbetonplatten mittels finiter Elemente. *Schweizerische Bauzeitung* **93**(20), 313–316.
- Dickens, J. G. and Jones, L. L. (1988). A general computer program for the yield-line solution of edge supported slabs. *Comput. Struct.* **30**(3), 465–476.
- Garvin, W. W. (1960). *Introduction to Linear Programming*. McGraw-Hill, New York.
- Jennings, A., Thavalingam, A., McKeown, J. J. and Sloan, D. (1994). On the optimisation of yield-line patterns. In *Developments in Computational Engineering Mechanics* (Edited by B. H. V. Topping), pp. 209–214. Civil-Comp Press, Edinburgh.
- Johansen, K. W. (1972). *Yield-line Formulae for Slabs*. Cement and Concrete Association, London.
- Munro, J. and Da Fonseca, A. M. A. (1978). Yield-line method by finite elements and linear programming. *Struct. Engineer* **56B**(2), 37–44.
- Wood, R. H. (1961). *Plastic and Elastic Design of Slabs and Plates*. Thames and Hudson, London.

## APPENDIX: JACOBIAN MATRICES

*Formation of  $J_{C_x}$* 

The derivatives required for the formation of the Jacobian matrix may be readily derived by noting that all the components in matrix **C** involve terms of the form  $a_i/h_i$  and it is therefore only necessary to obtain the derivatives of this type of function. Thus, for example,

$$\left(\frac{a_1}{h_1}\right) = \frac{(l_1^2 - l_2^2 + l_3^2)}{2[(y_1 - y_2)(x_3 - x_2) - (x_1 - x_2)(y_3 - y_2)]} = \frac{A_1}{H_1}$$

whence

$$\frac{\partial}{\partial x_1} \left(\frac{a_1}{h_1}\right) = \frac{H_1(x_3 - x_2) - A_1(y_2 - y_3)}{H_1^2} \quad (\text{A1})$$

Similarly,

$$\frac{\partial}{\partial x_2} \left(\frac{a_1}{h_1}\right) = \frac{H_1(2x_2 - x_1 - x_3) - A_1(y_3 - y_1)}{H_1^2} \quad (\text{A2})$$

and

$$\frac{\partial}{\partial x_3} \left(\frac{a_1}{h_1}\right) = \frac{H_1(x_1 - x_2) - A_1(y_1 - y_2)}{H_1^2} \quad (\text{A3})$$

The remaining derivatives with respect to the  $x$  coordinates may be obtained by appropriate cyclic permutation of the suffixes 1,2,3 and derivatives with respect to the  $y$  coordinates are obtained by  $x/y$  exchange.

*Formation of  $J_{f_x}$* 

The vector **f** comprises terms of the form  $ql_i/h_i/6$  and, taking a typical term,

$$\frac{\partial}{\partial x_1} \left(\frac{ql_1 h_1}{6}\right) = \frac{q}{6} \frac{\partial H_1}{\partial x_1} = \frac{q(y_2 - y_3)}{6} \quad (\text{A4})$$